Single-molecule and -particle spectroscopy in Leiden: absorption, scattering and fluorescence

Adhikari, S.; Orrit, M.A.G.J.

TOPICAL REVIEW

Single-molecule and -particle spectroscopy in Leiden: absorption, scattering and fluorescence

To cite this article: Subhasis Adhikari and Michel Orrit 2022 *J. Opt.* **24** 043001

IOP Publishing Journal of Optics
J. Opt. **24** (2022) 043001 (11pp) https://doi.org/10.1088/2040-8986/ac51b2

Topical Review

Single-molecule and -particle spectroscopy in Leiden: absorption, scattering and fluorescence

Subhasis Adhikari and Michel Orrit*

Huygens-Kamerlingh Onnes Laboratory, Leiden University, 2333 CA Leiden, The Netherlands

E-mail: Orrit@physics.leidenuniv.nl

Received 27 October 2021, revised 2 December 2021
Accepted for publication 3 February 2022
Published 21 February 2022

Abstract

Detection of single molecules or particles avoids ensemble averaging and thus is able to provide a very local heterogeneous information which is not available from an ensemble measurement. Single molecules or particles can be detected based on their three characteristic optical properties, absorption, scattering and fluorescence/photoluminescence, in addition to their label-free detection. This short review focuses on our group's research towards understanding and imaging the above three kinds of optical signals from single molecules and particles.

Keywords: single-molecule spectroscopy, single-particle spectroscopy, photothermal microscopy, plasmonic enhancement, label-free plasmonic sensor

(Some figures may appear in colour only in the online journal)

1. Introduction

In the past three decades, single-molecule (SM) and -particle spectroscopy has shown numerous applications in biological and nanomaterial sciences [1–10]. Single nanoobjects can be detected based on their absorption, scattering and fluorescence/ photoluminescence signals. In the last decade, our group has focused on understanding all these three optical properties of single molecules and particles either at low temperature or at room temperature. This review will focus on our group's work on these relevant topics in the past ten years.

The most commonly used method for detection of single molecules is fluorescence because of its ease of use and because it is background-free. One key advantage of SM fluorescence at low temperature is the very narrow linewidth of the zero-phonon line (ZPL) which can be used as an efficient sensor for minute changes in the molecule's environment, for example the detection of hopping of single electrons [11–14]. At room temperature, thermal fluctuations broaden the spectral linewidth, however single molecules can be spatially selected beyond the diffraction limit. One can use room-temperature SM fluorescence as a sensor for single-charge detection by looking at a single molecule's blinking dynamics induced by single charges hopping into and out of the molecule in electrochemically-controlled redox processes [15, 16]. One of the major limitations of SM fluorescence at room temperature is photobleaching, which restricts the range of excitation power used, and thus restricts SM observations to fluorophores with high quantum yields (QYs). Our group has shown that SM fluorescence can be enhanced in the presence of a simple metallic nanorod [16–23] and that SM fluorescence can also be detected for dye molecules with weak QYs with a good signal-to-noise ratio.

In contrast to fluorescent molecules, metallic nanoparticles are mostly detected by their scattering signals [24–27]. However, scattering is not background-free. Single metallic nanoparticles can also be detected efficiently by looking at

* Author to whom any correspondence should be addressed.

their background-free absorption and luminescence signals [7, 28–30]. Although the luminescence QY of single metallic nanospheres and nanorods are quite low, typically on the order of 10^{-6}, their large absorption cross sections enable detection of their luminescence with high contrast.

The most efficient method for detection of smaller-sized metallic nanoparticles is absorption, as it scales linearly with the particle's volume, in contrast to dark-field scattering, which scales quadratically with the particle's volume. Photothermal (PT) microscopy [7, 29, 31, 32] is able to measure absorption signals of particles with sizes below 40 nm, down to 1 nm. Typical media used for PT microscopy are organic liquids which have poor PT responses. Our group has used near-critical xenon to enhance the PT sensitivity by more than two orders of magnitude. This enabled us to study single multichromophoric systems at a low excitation power [33, 34]. PT microscopy also allows us to measure circular dichroism (CD) of a single chiral nanoobject with a high sensitivity [35]. In a label-free manner, single metallic nanoparticles can be used as plasmon sensors for the detection of single biomolecules [36]. Our recent study has demonstrated fast (sub-microsecond) label-free detection of single diffusing nanoparticles [37].

In this short review article, we discuss three major experimental techniques for detection of single particles or molecules: (a) fluorescence/ photoluminescence, (b) PT (i.e. absorption) and (c) scattering. In this regard, we recommend several articles [38–57], mostly reviews, by other groups about these three different techniques and their applications. Nevertheless, here we briefly describe the principles of these three methods. When a particle or molecule is excited by a photon, it absorbs the photon and enters an excited state. From the excited state, the molecule or the particle relaxes back to the ground state via either radiative or non-radiative processes. The radiative decay leads to Stoke-shifted fluorescence or photoluminescence, and to weaker anti-Stokes emission, which can be significant and useful for metal nanoparticles. As the fluorescence has different wavelengths from the excitation, it can be separated with high efficiency from the excitation by means of suitable spectral filters. Therefore, fluorescence is virtually background-free. The interaction of the molecule or the particle with the excitation beam also creates scattered light. This scattering can be detected via either dark-field or bright-field microscopy. In dark-field microscopy, the scattered light is detected in special configurations where no background excitation light is detected and thus, the method is ideally background-free. However, dark-field microscopy is limited to higher particle sizes compared to bright-field microscopy. In bright-field microscopy, the scattered light interferes with the reflected or the transmitted excited photons in the backward or the forward directions, respectively. In so-called interference scattering microscopy (iSCAT), the background signal is carefully subtracted from the interference signal. In contrast to fluorescence or scattering microscopy, PT microscopy is a two-color technique. When a metal nanoparticle or a molecule is excited by a heating laser, and relaxes from the excited state to the ground state non-radiatively, the relaxation creates heat surrounding the particle. This heat diffuses in the surrounding medium, creating a thermal lens. A second laser is used to probe the resulting perturbation. This probe beam is scattered by the thermal lens and interferes with the reflected or the transmitted probe beam, in a way similar to the interference in the iSCAT method. In PT microscopy, the background is removed through high-frequency modulation of the heating beam and detection of the interference signal with a sensitive lock-in detection. PT microscopy measures the absorption of a single particle or a molecule.

2. Low-temperature single-molecule fluorescence spectroscopy

Soon after the first detection of SM fluorescence at a cryogenic temperature [1], SM spectroscopy was extended to various fields of science, from soft-matter physics to biology [3]. We focus here on our group's work on cryogenic SM fluorescence experiments to investigate host-matrix-induced linear Stark effect of a single centrosymmetric organic dye molecule at 1.2 K.

2.1. Matrix-induced linear Stark effect of a single organic molecule at low temperature

The so-called Stark effect is the shift of spectral line of a molecule caused by an applied static electric field. This shift depends on the static dipole moment and polarizability of the molecule. At liquid-helium temperatures, the ZPL of an organic dye molecule is often lifetime-limited (with a linewidth of a few tens of MHz). For example, dibenzoterrylene (DBT) in a matrix of 2,3 dibromonaphthalene (DBN) has a linewidth of about 40 MHz [13]. Such a system is an efficient sensor of applied electric fields. A centrosymmetric molecule such as DBT in free space does not show any linear Stark effect due to the absence of a net permanent dipole moment. However, at cryogenic temperatures, the host matrix can break the centrosymmetry of the guest molecule's structure, which results in a net permanent dipole moment. Moradi *et al* [13] have reported that DBT molecules in DBN crystal at 1.2 K have large linear Stark effect due to symmetry breaking by the host matrix. Quantum chemistry simulations show that one DBT guest molecule replaces three DBN host molecules along the *a*-axis of the crystal, whereby the DBT molecule gains a net permanent dipole moment of 1.53 D, which is larger than the dipole moment of an isolated DBT molecule in its crystal-deformed geometry (i.e. 0.69 D). These authors have found that the absolute values of linear Stark coefficients of most molecules were narrowly distributed around 1.5 GHz $(\text{kV cm}^{-1})^{-1}$ when the electric field was aligned to the *a*-axis of the crystal, whereas their signs depend on which DBN molecules in the unit cell they substituted.

This strategy of using an asymmetric host molecule and lattice to create a large linear Stark-effect of a centro-symmetric molecule opens a new pathway to explore many other host-guest systems. A single organic dye molecule with a large linear Stark coefficient is an excellent probe for quantum-optical applications. It is important to mention here that not

all organic dye molecules are photostable (free from photoblinking) and spectrally stable (free from spectral diffusion) at cryogenic temperatures. Photostability, however, is a requirement for nanophotonics applications. DBT is an excellent guest molecule because of its high QY, its lifetime-limited ZPL and its high photostability. DBT in DBN host-guest system is therefore a very well-suited system for single-electron (or -charge) detection in such interesting devices as single-electron transistors.

3. Room temperature single-molecule fluorescence spectroscopy

In past three decades, SM fluorescence spectroscopy at room temperature has advanced fundamental understanding and spawned diverse applications of nanomaterials and of biological systems. Photoblinking, a characteristic fingerprint of a single molecule, is one of the cornerstones of superresolution fluorescence microscopy [38]. SM fluorescence can also be used as a sensor for studying electrochemistry at the SM level [15].

3.1. Single-electron transfer in a single Azurin protein molecule

Pradhan *et al* [15] have shown that single electron transfer events of single protein molecules can be studied in detail by monitoring changes of the fluorescence intensity and lifetime of a labeled fluorescent molecule (figure 1). The fluorescent molecule attached to an Azurin protein undergoes quenching in the oxidized form of the protein through fluorescence resonance energy transfer. The reduced form of the protein, however, does not absorb the dye fluorescence, and consequently no fluorescence quenching occurs in the reduced state. By analyzing blinking in time traces of the fluorescence signal, detailed statistics of single-electron transfer processes can be obtained at the single-protein level. The quenching process was confirmed by measuring the fluorescence lifetime of the labeled dye molecule in its dark state which was found to be 0.6 ns, indicating 90% fluorescence quenching. The bright and dark times of blinking events were dependent on the concentrations of ferri- (FeIII) and ferro (FeII) cyanate ions, which provided direct access to the electron transfer rates. Autocorrelation of bright and dark times indicated that electron transfer rates fluctuate over time, i.e. it demonstrated dynamical heterogeneity with a correlation time of hundreds of seconds. Abrupt changes of the correlation times over time were most probably due to the conformational changes of the protein molecule.

This study showed that single-electron transfer processes on a single small protein molecule of only 14 kDa can be studied using SM fluorescence microscopy. Studies by other groups have also shown that electrochemistry can be observed at the SM level using fluorescence spectroscopy [58, 59]. These studies indicate that a single fluorescent molecule can be used as a sensor for single-electron detection at room temperature.

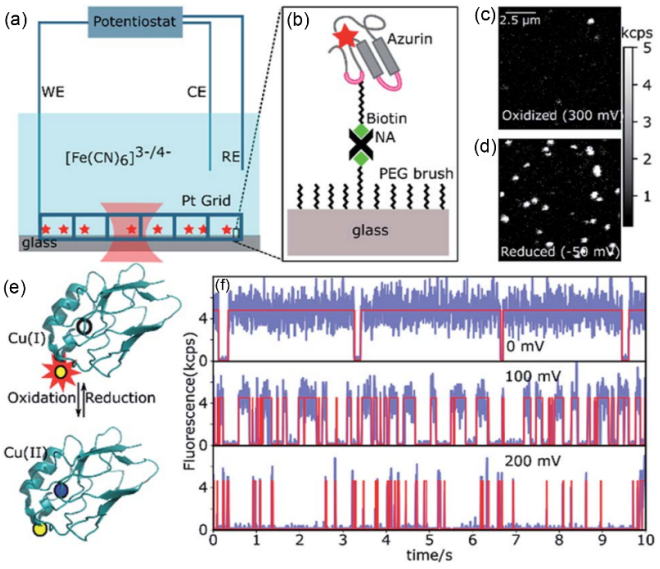

Figure 1. (a) Schematic of the electrochemical setup used by Pradhan *et al* [15]. Details of the setup are described in [15]. (b) Schematic of immobilization of protein molecule on the glass surface. (c), (d) Scanning confocal fluorescence image of the same area at oxidative (300 mV) and reductive (−50 mV) electrochemical potential indicating the change of fluorescence signal by single-molecule electrochemistry. (e) Schematic of oxidation-reduction of copper (Cu) of Azurin protein (empty dot in top and blue dot in bottom). The dye molecule (yellow dot) in its bright state (red star at top) and in its quenched state (in bottom). (f) Three timetraces at three different indicated potentials, showing the change of bright and dark times at different potentials. (a)–(f) Reproduced from [15] with permission of The Royal Society of Chemistry.

4. Enhanced single-molecule fluorescence spectroscopy

SM fluorescence spectroscopy is limited to a very restricted class of fluorescent dye molecules with high QYs. In the following, we outline our group's research towards enhancing fluorescence using a metallic nanostructure [17–23].

4.1. Single-molecule fluorescence enhancement near a single gold nanorod

Compared to nanofabricated metallic nanostructures, chemically synthesized gold nanorods have several advantages: (a) they do not require any expensive nanofabrication, (b) gold nanorods are often single-crystalline, whereas fabricated nanostructures are mostly poly-crystalline, which adds a damping channel for their surface plasmon and (c) gold nanorods have a strong surface plasmon polarized along their long axis, the longitudinal mode. The fluorescence of a single molecule is strongly enhanced when the molecule approaches the tip of a gold nanorod. The fluorescence enhancement is due to two factors: (a) excitation is enhanced by a combination of resonance with the longitudinal plasmon and of geometrical lighting rod effect; (b) emission is also enhanced by the Purcell effect, i.e. the enhanced density of photon states

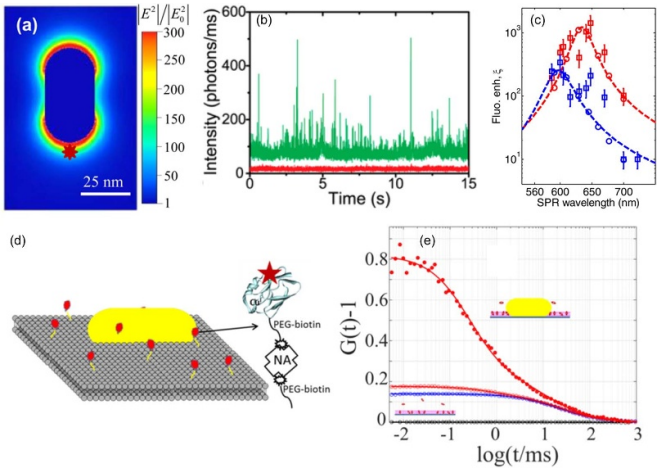

Figure 2. (a) Calculated near-field intensity map around a single gold nanorod of 47 nm length and 25 nm width. The surface plasmon resonance of the rod is at 629 nm and the excitation wavelength is 633 nm. The excitation is along the nanorod's long axis. (b) Fluorescence time traces of crystal violet molecules in the presence (green) and absence (red) of a single gold nanorod showing a large enhancement of fluorescence signal. (c) The maximum fluorescence enhancement factor as a function of surface plasmon resonance (SPR) wavelength for 11 single nanorods. Blue squares: excitation at 594 nm; red squares: excitation at 633 nm; open circles: theoretical calculation. The dotted solid lines are guides to the eye. (a)–(c) Reprinted with permission from [21]. Copyright (2014) American Chemical Society. (d) Schematic of a protein labeled with a dye molecule anchored on the bilayer surface. The Azurin protein labeled with Atto647N and biotin binds to 1, 2-Distearoyl-sn-glycero-3-phosphoethanolamine-Poly(ethylene glycol)-biotin (DSPE-PEG-biotin) in the bilayer through neutravidin (NA). (e) Autocorrelation of fluorescence signal of single dye-labeled protein molecules in the absence (blue open circles) and presence (red open circles) of a single gold nanorod. Solid red circles: autocorrelation of enhanced photons after lifetime filtering, showing much higher contrast than without lifetime filtering. (d), (e) Reprinted with permission from [19]. Copyright (2016) American Chemical Society.

able to receive the emitted photon. The emission process, however, is out-competed by fluorescence quenching when the molecule is very close (typically below 5 nm) to the nanorod's tip. Yuan *et al* [23] reported that the fluorescence signal of a single weakly fluorescent molecule, crystal violet, whose QY was 0.016, can be enhanced up to more than 1100 times (figure 2). Using a discrete-dipole approximation (DDA) simulation, Khatua *et al* [21] have found that the total enhancement factor of 1100 is a combination of excitation enhancement factor of about 130 times and emission enhancement factor of about 8.6 times. They have found that the fluorescence enhancement strongly depends on the overlap of the excitation laser and of the molecule's emission spectra with the surface plasmon spectra of the nanorod, and consequently on the surface plasmon resonance (SPR) of each single gold nanorod. The emission enhancement was associated with a significant shortening of the fluorescence lifetime.

One of the advantages of SM fluorescence enhancement for biomedical applications is that biomolecules labeled with fluorescent dyes can be studied at a very high concentration using fluorescence correlation spectroscopy (FCS) owing to the very small near-field volume around the gold nanorod's tip. Pradhan *et al* [19] have shown that the so-called enhanced FCS was not only restricted to dye molecules with weak QYs but can also be used for fluorophores with high QYs (figure 2). Enhanced FCS of dye molecules with high QYs at a high (micromolar) concentration was possible provided fluorescence bursts with shortened fluorescence lifetime were selected on the basis of their fluorescence lifetime. Indeed, enhanced emitted photons stem exclusively from the near-field of the gold nanorod. Such a selection enhances the contrast of the FCS curve even though the concentration of dye molecules was very high. Enhanced FCS may suffer from high background coming from dye molecules sticking on the glass surface. Pradhan *et al* [19] functionalized the glass surface with a lipid bilayer which prevented the molecules from sticking to the glass substrate. Bilayer-mediated surface functionalization is currently used in a number of biological applications. Pradhan *et al* [19] further demonstrated that single fluorescently-labeled Azurin proteins diffuse freely near a gold nanorod, without sticking to the bilayer surface. Autocorrelation of enhanced photons confirmed that the size of the near-field is about 10 times smaller than the diffraction-limited confocal diameter.

Zhang *et al* [18] have demonstrated that the enhancement factor can be more than four orders of magnitude for the case of two-photon excitation of dye molecules as the two-photon absorption rate scales quadratically with the near-field intensity. Two-photon excitation is currently used for studying biological systems because of a weaker scattering of infrared light by biological tissue and of the advantage of optical sectioning. Zhang *et al* [18] have achieved an enhancement factor of 15 000 using circularly polarized excitation (60 000 with linearly polarized excitation of the longitudinal plasmon). Due to the very high enhancement factor, the excitation laser power must be kept low to prevent heat-induced reshaping of the nanorods.

Enhanced FCS is a promising technique for studying many bio-molecular processes with a better contrast and higher concentrations of biomolecules. Fluorescence enhancement so far has been investigated only at a room temperature. SM spectroscopy at cryogenic temperatures would presumably provide a more detailed understanding of the enhancement mechanism, as the same molecule could be monitored for unlimited durations owing to the absence of photobleaching. Moreover, one could study many molecules in the near field simultaneously, thanks to spectral selection by the excitation laser. The accuracy of superresolution localization microscopy could also be improved due to enhancement of total number of emitted photons. Unfortunately, however, such experiments have remained elusive so far.

5. Single-particle photoluminescence spectroscopy

Two major limitations of SM fluorescence spectroscopy are photoblinking and photobleaching. In contrast to organic fluorescent dye molecules, metal nanoparticles are highly photostable, neither blink nor bleach even at a very high excitation

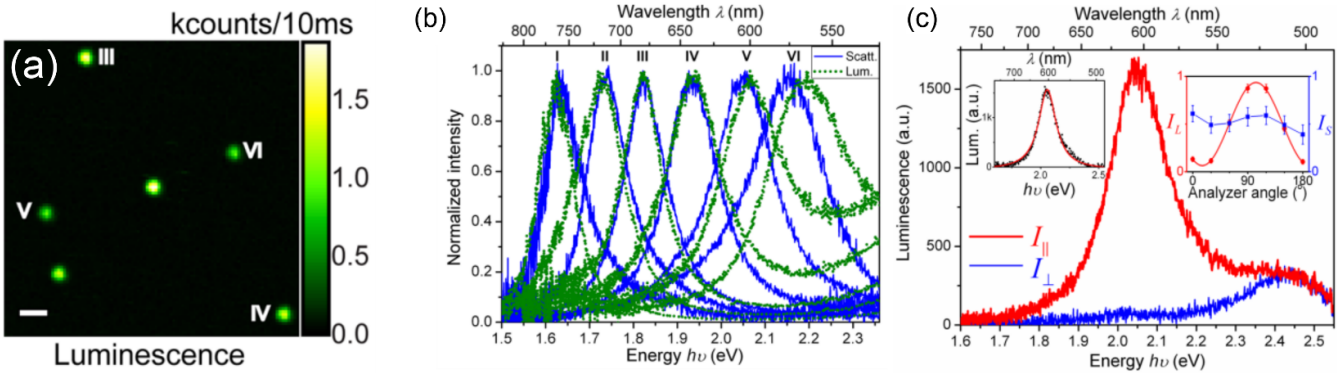

Figure 3. (a) photoluminescence image of single gold nanorods. (b) The photoluminescence (green) and scattering (blue) spectra of individual gold nanorods as marked in the image in (a). (c) Photoluminescence spectra of a single nanorod excited with a circularly polarized 476 nm laser and detected with a detection polarizer parallel (red) and perpendicular (blue) to the long axis of the nanorod. (Left inset) the longitudinal mode of the luminescence spectra with a Lorentzian fit and (right inset) detection polarization dependent photoluminescence signal of the longer (red) and shorter (blue) wavelength peaks of the luminescence spectra. (a)–(c) Reprinted with permission from [28]. Copyright (2012) American Chemical Society.

power. In addition, metal nanoparticles have shape-dependent optical properties. Compared to other metallic and semiconducting nanoparticles, gold nanoparticles are bio-compatible and non-toxic (We should mention here that the toxicity of gold nanoparticles is a subject of debate. We refer here a review by Alkilany and Murphy [60]). Although gold nanoparticles are mostly used as nano-absorbers or nano-scatterers, photoluminescence of gold nanoparticles can be used for imaging in biological systems. We would like to emphasize here that even though fluorescent molecules are less photostable than gold nanoparticles, fluorescent molecules are mostly used in biological studies because of their much smaller size and their easy, specific, one-to-one conjugation to biomolecules.

In the following, we discuss our group's work on understanding the photoluminescence signal of single gold nanorods and its application to a study of supercooled glycerol.

5.1. Photoluminescence of single gold nanorods

The photoluminescence QY of gold nanospheres ranging from 5 nm to 80 nm in size is about 10^{-7}, whereas the QY of gold nanorods is 10 times higher than that of gold nanospheres [28, 30]. Although the QY is very low, the large absorption cross section of metal nanoparticles compensates their weak QY. Yorulmaz *et al* [28] have found that the luminescence spectra of a single gold nanorod resembled the scattering spectra (figure 3). The match between luminescence and scattering spectra indicated that the surface plasmon of nanoparticles plays an essential part in their photoluminescence. The same authors also found that the luminescence spectra consist of two peaks—a shorter wavelength peak which is mainly due to the interband transition enhanced by the transverse plasmon, and a longer-wavelength peak which is due to the longitudinal plasmon. The photoluminescence signal at longer wavelength was found to be strongly polarized. Similar to gold nanospheres, the QY of gold nanorods is nearly independent of the SPR wavelength. However, at wavelengths shorter than 650 nm, the QY decreases due to the contribution of interband transitions.

5.2. Dynamical heterogeneity of supercooled glycerol probed by single gold nanorods

The polarized nature of the photoluminescence of a single nanorod can be exploited to track the rotational dynamics of the nanorod in a soft matter system. Compared to fluorescent dye molecules, gold nanorods have clear advantages—(a) nanorods are highly photostable and can be probed over very long periods of time and (b) nanorods, being large in size, can probe relaxation times of a heterogeneous system on a different length and timescales than a single fluorescent dye molecule [61, 62]. However, their main disadvantage is their size distribution, which must be accounted for. Yuan *et al* [63] have investigated the heterogeneous properties of a supercooled liquid, glycerol, near the critical temperature T_c by observing the temperature dependence of the rotational dynamics of a large gold nanorod. Single gold nanorods probed local viscosity of the glass-forming liquid. Yuan *et al* have found dynamical heterogeneity below 230 K, with a length scale of more than the length of the gold nanorod, i.e. over 30 nm. The heterogeneity below 230 K indicates the presence of cooperatively rearranging regions. The heterogeneity, however, disappears above 230 K, which qualitatively matches with the picture predicted by mode-coupling theory.

6. Gold nanoparticle as a heat source and temperature sensor

Metal nanoparticles are used as local heating sources for PT therapy [64, 65] because of their large absorption cross sections. The local temperature increase can create nanobubbles in a liquid, which can also be used for therapeutic applications [66]. When a metal nanoparticle absorbs a photon, an electron–hole pair is created. This electron–hole pair interacts with the thermal bath of the nanoparticle and gives rise to luminescence through radiative recombination, in addition to the much more frequent non-radiative relaxation. Inelastic interactions produce Stokes and anti-Stokes luminescence, red- and blue-shifted, respectively, from the

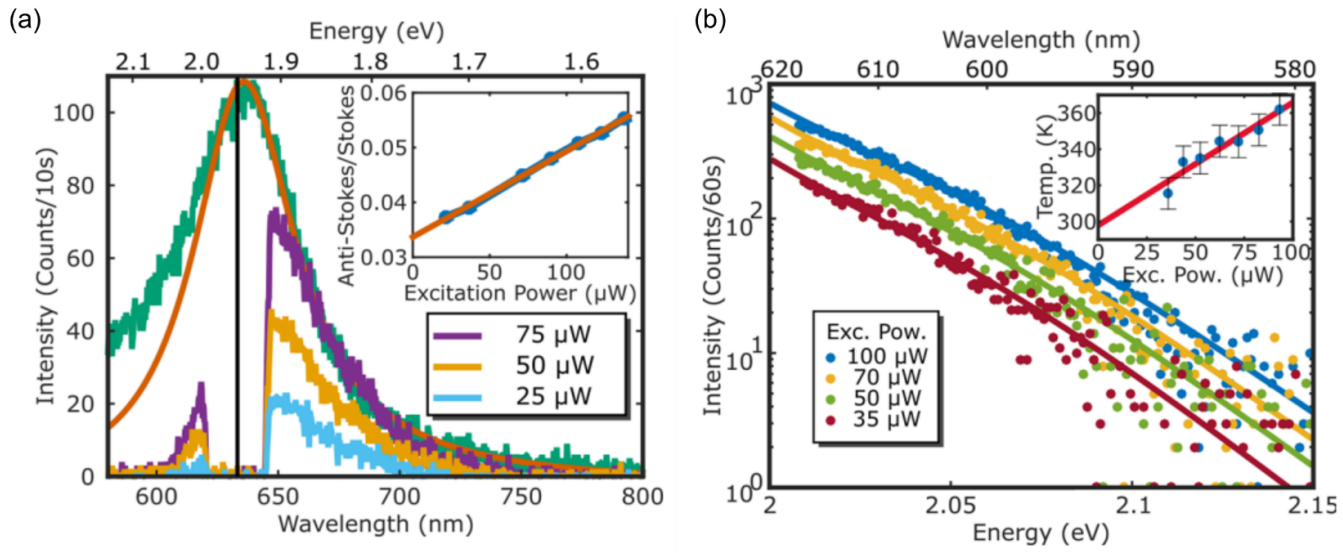

Figure 4. (a) Luminescence spectra of a single gold nanorod with excitation at 532 nm (green) and at 633 nm with different excitation powers (colors are indicated in inset). The solid orange curve is the surface plasmon spectrum extracted from the green curve. (Inset) Excitation power dependence of ratio of anti-Stokes and Stokes luminescence. (b) The anti-Stokes luminescence at different excitation powers fitted with a model discussed in the [11]. (Inset) The linear dependence of the calculated absolute temperature and the extrapolation to a temperature at zero excitation power which (296 K) is quite close to room temperature (293 K). Reproduced from [47].

excitation laser frequency. The anti-Stokes luminescence can be used as a nano-thermometer [67]. In the following, we briefly discuss our group's work in this area.

6.1. Nanobubble dynamics around a heated gold nanoparticle

Previously other groups have reported nanobubble formation using a pulsed excitation. Hou *et al* [68] have found that nanobubbles can also be formed using a continuous-wave excitation and that the formation of nanobubbles can be stabilized using a suitable heating intensity time profile. The nanobubbles were created only above a certain threshold excitation power. Below the threshold, no bubbles were formed. Hou *et al* have found that the nanobubble formation was explosive in nature with a rise time of about 15 ns and a decay time of about 30 ns. Such a fast dynamics could not be tracked with a lock-in amplifier, which is too slow. Hou *et al* [68] used a fast photodiode and a fast oscilloscope to measure the explosion of nanobubbles. The nanobubbles' formation showed a signature of acoustic echoes which arise from sound waves created by the initial explosion. A full theoretical understanding of the complex kinetics of nanobubbles still requires further investigation.

6.2. Gold nanoparticle as a nanoprobe for measurements of absolute temperature

As stated above, the shape of the photoluminescence spectrum of a metal nanoparticle bears the signature of interactions of the excited electron–hole pair(s) with the thermally excited charge carriers and phonons. The anti-Stokes side of the luminescence band is particularly sensitive to temperature, as it decays exponentially with frequency. Carattino *et al* [67] have demonstrated that the continuous-wave anti-Stokes luminescence of a gold nanoparticle can be used to measure absolute temperature of a medium without prior calibration (figure 4). By measuring the surface plasmon spectra of a gold nanorod and exciting the nanorod at the longitudinal plasmon, the anti-Stokes luminescence spectra provided information about the absolute temperature of the particle. Carattino *et al* found that the calculated absolute temperature scales linearly with excitation power and extrapolated to low power to calculate the temperature at zero excitation (i.e. ambient temperature).

Jollans *et al* [69] reported time-resolved anti-Stokes luminescence measurements with a pulsed excitation of a femtosecond laser. Ultrafast pump-probe spectroscopy allowed them to measure effective electron temperatures of 1000 K and ultrafast kinetics of excited electrons at picosecond timescales. The time-resolved spectra confirmed that the anti-Stokes side of the luminescence spectrum is more temperature-dependent than the Stokes side. Anti-Stokes luminescence can be applied to estimate the instantaneous and local electronic temperature.

7. Photothermal microscopy of single molecules and nanoparticles

The higher photostability of metal nanoparticles compared to single fluorescent dye molecules promises many applications in soft matter and biology [70–73]. Smaller-sized metal nanoparticles, typically below 40 nm, are difficult to detect by traditional dark-field scattering microscopy because scattering cross sections scale with the particle's squared volume. The absorption cross section of a metal nanoparticle scales linearly with volume. Therefore, the absorption of a small nanoparticle

is easier to measure than its (dark-field) scattering. When a metal nanoparticle is excited, the nanoparticle absorbs photons and the excited particle relaxes non-radiatively. The non-radiative relaxation creates heat surrounding the particle, and this heat eventually diffuses away into the surrounding medium. The ensuing refractive-index change is probed with a second laser by observing changes in the scattered intensity. This kind of pump-probe microscopy is known as PT microscopy [7, 32], also known as thermal-lens microscopy [74, 75]. The PT sensitivity depends on the coefficient of refractive-index change due to the change in temperature, i.e. the thermo-refractive coefficient. The typical thermo-refractive coefficient [29] of an organic liquid is in the order of 10^{-4} K^{-1}. Such a low thermo-refractive coefficient does not suffice to detect single organic dye molecules whose saturation intensity is low and which photobleach at high excitation power. To enhance PT sensitivity, Ding *et al* [33] have demonstrated that using near-critical xenon, the sensitivity can be enhanced more than two orders of magnitude. This high sensitivity allows detection of single organic fluorescent molecules at a comparatively low excitation power [34].

7.1. Absorption measurements of single conjugated polymers

Hou *et al* [34] have reported that absorption of single conjugated polymers of poly[2-methoxy-5-(2-ethylhexyloxy)-1,4-phenylenevinylene] (MEHPPV) can be imaged in near-critical xenon with a low excitation power of below 1 kW cm^{-2} (figure 5). By simultaneous measurements of absorption and fluorescence, the QY of a single conjugated polymer molecule can be determined, and detailed insight into the processes of inter- and intra-molecular energy transfer can be obtained. The QYs of single polymer molecules were found to be broadly distributed and to correlate with the polymer size (taking absorption as a proxy). The nonlinear correlation between the QY and the absorption cross section was assigned to fluorescence quenching by defects, which are more likely to occur in longer polymer chains. The fluorescence and absorption signals of a single chain photobleached continuously upon continuous excitation, with a faster bleaching rate for fluorescence than for absorption, indicating the creation of photo-induced trap states which quench fluorescence by intra-chain exciton migration. Further studies of correlative absorption and fluorescence spectroscopy of single conjugated polymer chains would provide a more detailed understanding of these non-radiative energy transfer processes.

7.2. Photothermal CD spectroscopy of single metal nanoparticles

CD is a property of a chiral nano-object which interacts differently with circularly polarized light of opposite handedness. CD is defined as the differential absorption of left- and right-circularly polarized light. The standard way to access the CD of a single chiral nanoparticle is to measure the differential extinction in a CD spectrometer. Alternatively, differential scattering can also be measured in a microscope [24, 76, 77]. Because it directly measures absorption,

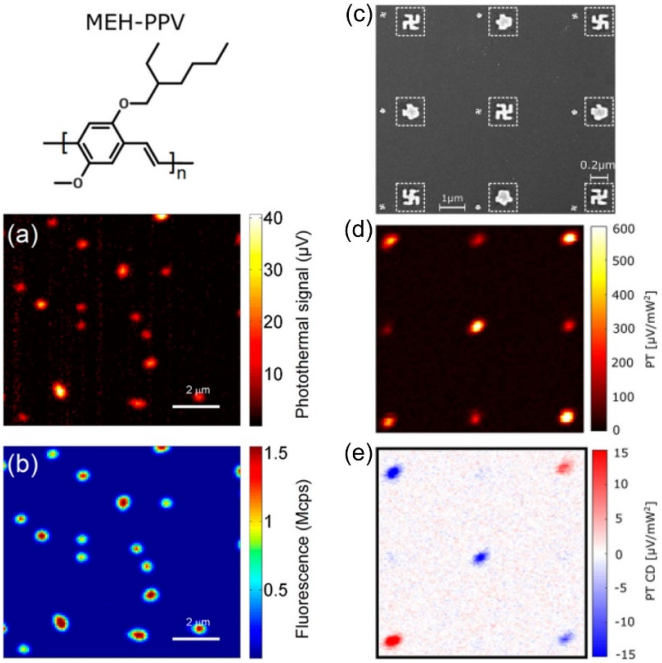

Figure 5. (Left) top: chemical structure of MEHPPV; (a) and (b): absorption and fluorescence images of single conjugated polymer chains in the same area, respectively. (a), (b) Reprinted with permission from [34]. Copyright (2017) American Chemical Society. (Right) (c) scanning electron microscopy (SEM), (d) photothermal (PT) and (e) photothermal circular dichroism (PTCD) images of single three left-handed and two right-handed chiral gammadion structures and four achiral nanostructures. (c)–(e) Reprinted with permission from [35]. Copyright (2019) American Chemical Society.

PT microscopy provides direct access to the CD signal of a single chiral nanoparticle, free from scattering or extinction contributions. Spaeth *et al* [35] have proposed photothermal circular dichroism microscopy, and illustrated it with CD images of single metallic nanoparticles with g-factors down to 10^{-3} within an integration time of 30 ms. In their method, Koehler illumination by circularly polarized heating light guarantees an excellent polarization quality, which would be very difficult to ensure with a tightly focused illumination. The high spatial resolution was provided by the high-neutravidin (NA) probing beam, which was diffraction-limited but unpolarized. As a proof-of-concept, Spaeth *et al* have demonstrated enantio-selection of single metallic gammadion structures with a g-factor sensitivity of 0.004 with an integration time of 30 ms (figure 5). Because of the high sensitivity, they were also able to detect very weak CD signals of g-factor below 10^{-3} for quasi-spherical gold nanoparticles.

8. Label-free plasmon-sensing using a single gold nanorod

Optical probing of single molecules or nanoparticles in a label-free manner has been a great topic of research in the past two decades [6]. Our group has focused on label-free probing of single molecules using a single gold nanorod as

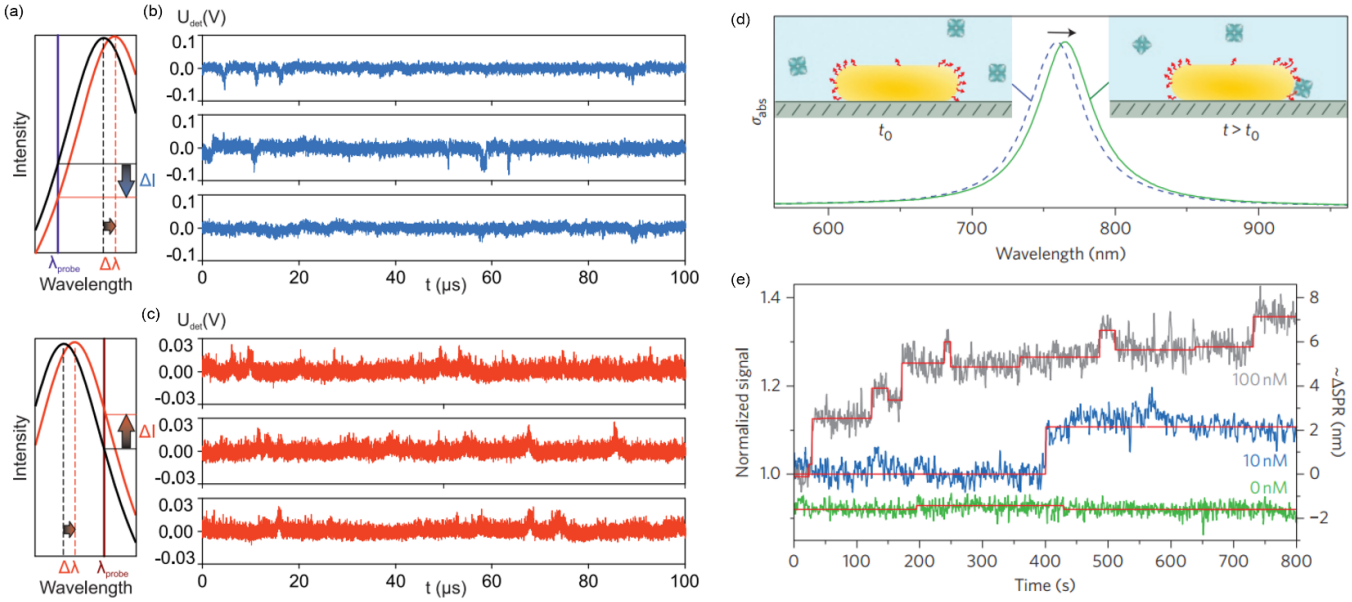

Figure 6. (a)–(c): Label-free single particle detection and (d) and (e): label-free single-molecule detection. (a) Schematic representation of the plasmon red-shift by a refractive particle. The plasmon shift is monitored with a laser in the blue wing (top) or the red wing (bottom) of a nanorod's longitudinal plasmon. (b), (c) Scattering intensity time traces of a single gold nanorod presenting intensity fluctuations due to single 5 nm gold nanoparticles traversing the near field (top (bottom) the plasmon is probed on the blue (red) wing). (a)–(c) Reprinted with permission from [37]. Copyright (2020) American Chemical Society. (d) Scheme of a single gold nanorod functionalized with biotin molecules specifically at the tip of the rod. A red shift follows from the binding of a single protein molecule to the rod tip. (e) Time traces of photothermal signals (left axis) and plasmon shift (right axis) of a single gold nanorod in the presence of single protein molecules at three different concentrations, indicating the binding of single protein molecules. The red lines are fits using a step-finding algorithm. (d), (e) Reprinted by permission from [36]. Copyright (2012) Springer Nature Customer Service Center GmbH.

a plasmon sensor. Ziljstra *et al* [36] demonstrated that binding and unbinding of a single protein molecule to a single gold nanorod can be detected using PT microscopy by looking at the plasmon shift of the longitudinal SPR at a single frequency. The plasmon shift is due to the change of the local refractive index upon binding of the protein molecule. The near-field is strongest at the tip of the rod and therefore the strongest plasmon shift occurs when the protein molecules bind to the tip of the rod. By selective functionalization, Ziljstra *et al* were able to bind the protein molecules specifically to the tip of the nanorod. The binding and unbinding events were observed by step-wise changes of PT signal as shown in figure 6. The high sensitivity of the method allows sensing single protein molecules with molecular weight of 53 kDa. The method is promising for label-free detection of single biomolecules, possibly even inside cells. Baaske *et al* [37] developed a scattering-based method for probing single molecules using plasmon sensing with a sub-microsecond time resolution which is 10 000 times faster than in previous reports. Using the characteristic polarization anisotropic scattering of a single gold nanorod, the signal-to-noise can be optimized by choosing the proper angle of the excitation polarization and the Gouy phase. Scattering contribution from direct analyte particles can be neglected in a cross-polarized configuration. Baaske *et al* have demonstrated detection of single 5 nm gold nanoparticles in a label-free manner (figure 6), predicting the detection of single protein molecules with a molecular weight of 20 kDa and an integration time of 10 ns.

9. Rotational and translational Brownian motion of a hot gold nanorod in an optical trap

Metal nanoparticles are more polarizable than dielectric particles and can be trapped in an optical trap for smaller sizes. However, residual heating of the metal by intense trap light requires special precautions and is reduced by shifting the trapping light to near IR, typically 1064 nm. The stable trapping of smaller-sized gold nanoparticles and quantitative measurements of optical torque acting on anisotropic particles could enable SM experiments in biological systems. Ruijgrok *et al* [78] have demonstrated that both translational and rotational motion of a gold nanorod in an optical trap can be studied simultaneously by observing the fluctuations of the polarization-dependent scattered signal. The autocorrelation of scattered signals provided information about hot Brownian motion [79] i.e. Brownian motion of a heated nanoobject in an inhomogeneous temperature and viscosity profile. The autocorrelation was found to be bi-exponential, consisting of fast rotational and slower translational dynamics. Because of the different ranges of the velocity field for translational and rotational dynamics, the effective fluid viscosities are different for translational and rotational dynamics. The maximum

torque measured for a single gold nanorod of 60 nm long and 25 nm diameter was about 100 pN nm. Such a torque is large enough to study many SM processes in biological systems.

10. Magnetic susceptibility of single gold nanorods

Even though bulk gold is diamagnetic in nature, gold nanoparticles with functionalized ligands can show magnetic properties. Our group have focused on measuring the magnetic alignment in suspensions of gold nanorods by linear dichroism and linear birefringence. Van Rhee *et al* [80] reported that gold nanorods show a temperature-independent diamagnetic behavior, at least up to 300 K. Although measurements were not performed above 300 K, it is most likely that gold nanorods would keep their strong diamagnetic behavior well above this temperature. The alignment allowed Van Rhee *et al* to calculate the magnetic susceptibility of gold nanorods, which was found to be in the order of 10^{-6}–10^{-7}, three orders of magnitude higher than that of bulk gold. The magnetization depended linearly on the magnetic field. The enhanced magnetic susceptibility was attributed to the orbital magnetic moment of electrons in the gold core.

11. Summary

This review discusses several key research works of our group in past ten years in the topic of SM and single-particle spectroscopy. Here are some key highlights:

(a) We have shown that a single molecule can be used as an efficient sensor for single electron detection at a low temperature using linear Stark effect.
(b) At room temperature, a single molecule can also be used as a sensitive sensor for single charge detection using its electric-field induced fluorescence properties.
(c) SM fluorescence can be enhanced by more than thousand times in the presence of a metallic nanorod due to plasmonic enhancement.
(d) In contrast to scattering, single metallic nanoparticles can be efficiently detected by background-free methods, absorption and photoluminescence.
(e) Anti-Stokes luminescence of a metallic nanoparticle allows to measure absolute temperature surrounding a nanoparticle.
(f) Absorption measurements of a single metallic nanoparticle allow to measure CD down to the single-particle level.
(g) Single metallic nanorod is an efficient plasmonic sensor for label-free single molecule detection with a submicrosecond time resolution.
(h) The optical torque acting on a metal nanoparticle in an optical trap can be measured by studying the Brownian motion of the particle in the trap and could be used in single-biomolecule experiments.

Data availability statement

No new data were created or analyzed in this study.

Acknowledgment

The work summarized in this review was financed almost entirely by the Netherlands Organization for Scientific Research (NWO), which is gratefully acknowledged.

ORCID iDs

Subhasis Adhikari https://orcid.org/0000-0002-0914-433X
Michel Orrit https://orcid.org/0000-0002-3607-3426

References

[1] Moerner W E and Kador L 1989 Optical detection and spectroscopy of single molecules in a solid *Phys. Rev. Lett.* **62** 2535–8
[2] Orrit M and Bernard J 1990 Single pentacene molecules detected by fluorescence excitation in a p-terphenyl crystal *Phys. Rev. Lett.* **65** 2716–9
[3] Moerner W E and Orrit M 1999 Illuminating single molecules in condensed matter *Science* **283** 1670–6
[4] Tamarat P, Maali A, Lounis B and Orrit M 2000 Ten years of single-molecule spectroscopy *J. Phys. Chem.* A **104** 1–16
[5] Kozankiewicz B and Orrit M 2014 Single-molecule photophysics, from cryogenic to ambient conditions *Chem. Soc. Rev.* **43** 1029–43
[6] Jollans T, Baaske M D and Orrit M 2019 Nonfluorescent optical probing of single molecules and nanoparticles *J. Phys. Chem.* C **123** 14107–17
[7] Adhikari S, Spaeth P, Kar A, Baaske M D, Khatua S and Orrit M 2020 Photothermal microscopy: imaging the optical absorption of single nanoparticles and single molecules *ACS Nano* **14** 16414–45
[8] Toninelli C *et al* 2021 Single organic molecules for photonic quantum technologies *Nat. Mater.* **20** 1615–28
[9] Orrit M, Ha T and Sandoghdar V 2014 Single-molecule optical spectroscopy *Chem. Soc. Rev.* **43** 973–6
[10] Basché T, Moerner W E, Orrit M and Wild U P 2008 *Single-Molecule Optical Detection, Imaging and Spectroscopy* (New York: Wiley)
[11] Nicolet A A L, Bordat P, Hofmann C, Kol'chenko M A, Kozankiewicz B, Brown R and Orrit M 2007 Single dibenzoterrylene molecules in an anthracene crystal: main insertion sites *ChemPhysChem* **8** 1929–36
[12] Deperasińska I, Karpiuk E, Banasiewicz M and Kozankiewicz B 2010 On the photo-stability of single molecules. Dibenzoterrylene in 2,3-dimethylnaphthalene crystals *Chem. Phys. Lett.* **492** 93–97
[13] Moradi A, Ristanović Z, Orrit M, Deperasińska I and Kozankiewicz B 2019 Matrix-induced linear Stark effect of single dibenzoterrylene molecules in 2,3-dibromonaphthalene crystal *ChemPhysChem* **20** 55–61
[14] Colautti M, Piccioli F S, Ristanović Z, Lombardi P, Moradi A, Adhikari S, Deperasinska I, Kozankiewicz B, Orrit M and Toninelli C 2020 Laser-induced frequency tuning of Fourier-limited single-molecule emitters *ACS Nano* **14** 13584–92

[15] Pradhan B, Engelhard C, Mulken S V, Miao X, Canters G W and Orrit M 2020 Single electron transfer events and dynamical heterogeneity in the small protein Azurin from pseudomonas aeruginosa *Chem. Sci.* **11** 763–71

[16] Zhang W, Caldarola M, Pradhan B and Orrit M 2017 Gold nanorod enhanced fluorescence enables single-molecule electrochemistry of methylene blue *Angew. Chem., Int. Ed.* **56** 3566–9

[17] Lu X, Ye G, Punj D, Chiechi R C and Orrit M 2020 Quantum yield limits for the detection of single-molecule fluorescence enhancement by a gold nanorod *ACS Photonics* **7** 2498–505

[18] Zhang W, Caldarola M, Lu X and Orrit M 2018 Plasmonic enhancement of two-photon-excited luminescence of single quantum dots by individual gold nanorods *ACS Photonics* **5** 2960–8

[19] Pradhan B, Khatua S, Gupta A, Aartsma T, Canters G and Orrit M 2016 Gold-nanorod-enhanced fluorescence correlation spectroscopy of fluorophores with high quantum yield in lipid bilayers *J. Phys. Chem.* C **120** 25996–6003

[20] Khatua S, Yuan H and Orrit M 2015 Enhanced-fluorescence correlation spectroscopy at micro-molar dye concentration around a single gold nanorod *Phys. Chem. Chem. Phys.* **17** 21127–32

[21] Khatua S, Paulo P M R, Yuan H, Gupta A, Zijlstra P and Orrit M 2014 Resonant plasmonic enhancement of single-molecule fluorescence by individual gold nanorods *ACS Nano* **8** 4440–9

[22] Khatua S and Orrit M 2014 Probing, sensing, and fluorescence enhancement with single gold nanorods *J. Phys. Chem. Lett.* **5** 3000–6

[23] Yuan H, Khatua S, Zijlstra P, Yorulmaz M and Orrit M 2013 Thousand-fold enhancement of single-molecule fluorescence near a single gold nanorod *Angew. Chem., Int. Ed.* **52** 1217–21

[24] Al-Zubeidi A, McCarthy L A, Rafiei-Miandashti A, Heiderscheit T S and Link S 2021 Single-particle scattering spectroscopy: fundamentals and applications *Nanophotonics* **10** 1621–55

[25] Zijlstra P and Orrit M 2011 Single metal nanoparticles: optical detection, spectroscopy and applications *Rep. Prog. Phys.* **74** 106401

[26] M A V D, Tchebotareva A L, Orrit M, Lippitz M, Berciaud S, Lasne D, Cognet L and Lounis B 2006 Absorption and scattering microscopy of single metal nanoparticles *Phys. Chem. Chem. Phys.* **8** 3486–95

[27] van Dijk M A, Lippitz M and Orrit M 2005 Far-field optical microscopy of single metal nanoparticles *Acc. Chem. Res.* **38** 594–601

[28] Yorulmaz M, Khatua S, Zijlstra P, Gaiduk A and Orrit M 2012 Luminescence quantum yield of single gold nanorods *Nano Lett.* **12** 4385–91

[29] Gaiduk A, Ruijgrok P V, Yorulmaz M and Orrit M 2010 Detection limits in photothermal microscopy *Chem. Sci.* **1** 343–50

[30] Gaiduk A, Yorulmaz M and Orrit M 2011 Correlated absorption and photoluminescence of single gold nanoparticles *ChemPhysChem* **12** 1536–41

[31] Selmke M, Braun M and Cichos F 2012 Photothermal single-particle microscopy: detection of a nanolens *ACS Nano* **6** 2741–9

[32] Boyer D, Tamarat P, Maali A, Lounis B and Orrit M 2002 Photothermal imaging of nanometer-sized metal particles among scatterers *Science* **297** 1160–3

[33] Ding T X, Hou L, Meer H V D, Alivisatos A P and Orrit M 2016 Hundreds-fold sensitivity enhancement of photothermal microscopy in near-critical xenon *J. Phys. Chem. Lett.* **7** 2524–9

[34] Hou L, Adhikari S, Tian Y, Scheblykin I G and Orrit M 2017 Absorption and quantum yield of single conjugated polymer poly[2-methoxy-5-(2-ethylhexyloxy)-1, 4-phenylenevinylene] (MEH-PPV) molecules *Nano Lett.* **17** 1575–81

[35] Spaeth P, Adhikari S, Le L, Jollans T, Pud S, Albrecht W, Bauer T, Caldarola M, Kuipers L and Orrit M 2019 Circular dichroism measurement of single metal nanoparticles using photothermal imaging *Nano Lett.* **19** 8934–40

[36] Zijlstra P, Paulo P M R and Orrit M 2012 Optical detection of single non-absorbing molecules using the surface plasmon resonance of a gold nanorod *Nat. Nanotechnol.* **7** 379–82

[37] Baaske M D, Neu P S and Orrit M 2020 Label-free plasmonic detection of untethered nanometer-sized Brownian particles *ACS Nano* **14** 14212–8

[38] Moerner W E 2015 Nobel lecture: single-molecule spectroscopy, imaging, and photocontrol: foundations for super-resolution microscopy *Rev. Mod. Phys.* **87** 1183–212

[39] Betzig E 2015 Single molecules, cells, and super-resolution optics (Nobel Lecture) *Angew. Chem., Int. Ed.* **54** 8034–53

[40] Young G *et al* 2018 Quantitative mass imaging of single biological macromolecules *Science* **360** 423–7

[41] Taylor R W and Sandoghdar V 2019 Interferometric scattering microscopy: seeing single nanoparticles and molecules via rayleigh scattering *Nano Lett.* **19** 4827–35

[42] Orrit M 2002 Single-molecule spectroscopy: the road ahead *J. Chem. Phys.* **117** 10938–46

[43] Sönnichsen C *et al* 2000 Spectroscopy of single metallic nanoparticles using total internal reflection microscopy *Appl. Phys. Lett.* **77** 2949–51

[44] Cheng J-X and Xie X S (eds) 2012 *Coherent Raman Scattering Microscopy* (Boca Raton, FL: CRC Press) (https://doi.org/10.1201/b12907)

[45] Fernée M J, Tamarat P and Lounis B 2014 Spectroscopy of single nanocrystals *Chem. Soc. Rev.* **43** 1311–37

[46] Reckmeier C J, Schneider J, Susha A S and Rogach A L 2016 Luminescent colloidal carbon dots: optical properties and effects of doping *Opt. Express* **24** A312–A340

[47] Lounis B and Orrit M 2005 Single-photon sources *Rep. Prog. Phys.* **68** 1129–79

[48] Vogelsang J, Kasper R, Steinhauer C, Person B, Heilemann M, Sauer M and Tinnefeld P 2008 A reducing and oxidizing system minimizes photobleaching and blinking of fluorescent dyes *Angew. Chem., Int. Ed.* **47** 5465–9

[49] Wöll D and Flors C 2017 Super-resolution fluorescence imaging for materials science *Small Methods* **1** 1700191

[50] Stratmann S A and van Oijen A M 2014 DNA replication at the single-molecule level *Chem. Soc. Rev.* **43** 1201–20

[51] Gahlmann A and Moerner W E 2014 Exploring bacterial cell biology with single-molecule tracking and super-resolution imaging *Nat. Rev. Microbiol.* **12** 9–22

[52] Roy R, Hohng S, Ha T and Practical A 2008 Guide to single-molecule FRET *Nat. Methods* **5** 507–16

[53] Lerner E, Cordes T, Ingargiola A, Alhadid Y, Chung S, Michalet X and Weiss S 2018 Toward dynamic structural biology: two decades of single-molecule förster resonance energy transfer *Science* **359** eaan1133

[54] Bailo E and Deckert V 2008 Tip-enhanced Raman scattering *Chem. Soc. Rev.* **37** 921–30

[55] Wang Q, Goldsmith R H, Jiang Y, Bockenhauer S D and Moerner W E 2012 Probing single biomolecules in solution using the anti-Brownian electrokinetic (ABEL) trap *Acc. Chem. Res.* **45** 1955–64

[56] Candelli A, Wuite G J L and Peterman E J G 2011 Combining optical trapping, fluorescence microscopy and micro-fluidics for single molecule studies of DNA–protein interactions *Phys. Chem. Chem. Phys.* **13** 7263–72

[57] Warning L A, Miandashti A R, McCarthy L A, Zhang Q, Landes C F and Link S 2021 Nanophotonic approaches for chirality sensing *ACS Nano* **15** 15538–66
[58] Chen P, Zhou X, Shen H, May Andoy N, Choudhary E, Han K-S, Liu G and Meng W 2010 Single-molecule fluorescence imaging of nanocatalytic processes *Chem. Soc. Rev.* **39** 4560–70
[59] Xu W, Kong J S, Yeh Y-T E and Chen P 2008 Single-molecule nanocatalysis reveals heterogeneous reaction pathways and catalytic dynamics *Nat. Mater.* **7** 992–6
[60] Alkilany A M and Murphy C J 2010 Toxicity and cellular uptake of gold nanoparticles: what we have learned so far? *J. Nanopart. Res.* **12** 2313–33
[61] Adhikari S, Selmke M and Cichos F 2011 Temperature dependent single molecule rotational dynamics in PMA *Phys. Chem. Chem. Phys.* **13** 1849–56
[62] Kulzer F, Xia T and Orrit M 2010 Single molecules as optical nanoprobes for soft and complex matter *Angew. Chem., Int. Ed.* **49** 854–66
[63] Yuan H, Khatua S, Zijlstra P and Orrit M 2014 Individual gold nanorods report on dynamical heterogeneity in supercooled glycerol *Faraday Discuss.* **167** 515–27
[64] Huang X and El-Sayed M A 2010 Gold nanoparticles: optical properties and implementations in cancer diagnosis and photothermal therapy *J. Adv. Res.* **1** 13–28
[65] Huang X, Jain P K, El-Sayed I H and El-Sayed M A 2007 Plasmonic photothermal therapy (PPTT) using gold nanoparticles *Lasers Med. Sci.* **23** 217
[66] Lapotko D 2009 Plasmonic nanoparticle-generated photothermal bubbles and their biomedical applications *Nanomedicine* **4** 813–45
[67] Carattino A, Caldarola M and Orrit M 2018 Gold nanoparticles as absolute nanothermometers *Nano Lett.* **18** 874–80
[68] Hou L, Yorulmaz M, Verhart N R and Orrit M 2015 Explosive formation and dynamics of vapor nanobubbles around a continuously heated gold nanosphere *New J. Phys.* **17** 013050
[69] Jollans T, Caldarola M, Sivan Y and Orrit M 2020 Effective electron temperature measurement using time-resolved anti-stokes photoluminescence *J. Phys. Chem.* A **124** 6968–76
[70] Leduc C, Si S, Gautier J, Soto-Ribeiro M, Wehrle-Haller B, Gautreau A, Giannone G, Cognet L and Lounis B 2013 A highly specific gold nanoprobe for live-cell single-molecule imaging *Nano Lett.* **13** 1489–94
[71] Leduc C, Jung J-M, Carney R R, Stellacci F and Lounis B 2011 Direct investigation of intracellular presence of gold nanoparticles via photothermal heterodyne imaging *ACS Nano* **5** 2587–92
[72] Lasne D, Blab G A, Berciaud S, Heine M, Groc L, Choquet D, Cognet L and Lounis B 2006 Single nanoparticle photothermal tracking (SNaPT) of 5-Nm gold beads in live cells *Biophys. J.* **91** 4598–604
[73] Cognet L, Tardin C, Boyer D, Choquet D, Tamarat P and Lounis B 2003 Single metallic nanoparticle imaging for protein detection in cells *Proc. Natl Acad. Sci.* **100** 11350–5
[74] Kitamori T, Tokeshi M, Hibara A and Sato K © 2004 AMERICAN CHEMICAL SOCIETY 9
[75] Uchiyama K, Hibara A, Kimura H, Sawada T and Kitamori T 2000 Thermal lens microscope *Jpn. J. Appl. Phys.* **39** 5316
[76] Vinegrad E, Vestler D, Ben-Moshe A, Barnea A R, Markovich G and Cheshnovsky O 2018 Circular dichroism of single particles *ACS Photonics* **5** 2151–9
[77] Zhang Q *et al* 2019 Unraveling the origin of chirality from plasmonic nanoparticle-protein complexes *Science* **365** 1475–8
[78] Ruijgrok P V, Verhart N R, Zijlstra P, Tchebotareva A L and Orrit M 2011 Brownian fluctuations and heating of an optically aligned gold nanorod *Phys. Rev. Lett.* **107** 037401
[79] Rings D, Schachoff R, Selmke M, Cichos F and Kroy K 2010 Hot Brownian motion *Phys. Rev. Lett.* **105** 090604
[80] van Rhee P G, Zijlstra P, Verhagen T G A, Aarts J, Katsnelson M I, Maan J C, Orrit M and Christianen P C M 2013 Giant magnetic susceptibility of gold nanorods detected by magnetic alignment *Phys. Rev. Lett.* **111** 127202